

9. LATE PALEOCENE AND EARLY EOCENE CALCAREOUS NANNOFOSSILS FROM THREE BOREHOLES IN AN ONSHORE-OFFSHORE TRANSECT FROM NEW JERSEY TO THE ATLANTIC CONTINENTAL RISE¹

Laurel M. Bybell² and Jean M. Self-Trail²

ABSTRACT

Closely spaced, upper Paleocene and lower Eocene samples from three boreholes near Clayton, NJ, at Island Beach, NJ, and at Site 605 on the Atlantic Ocean continental rise were examined for their calcareous nannofossil content. This study documents calcareous nannofossil occurrences in Zones NP9 and NP10 and identifies biostratigraphically useful species, presents unexpected upbasin-downbasin distributional patterns of calcareous nannofossils, discusses the gradual evolutionary transition between two calcareous nannofossil species, and clarifies the relationship between the genera *Rhomboaster* and *Tribrachiatus*. One new species, *Rhomboaster weii*, is described, and two new combinations, *Blackites herculesii* and *Rhomboaster digitalis*, are established.

INTRODUCTION

As part of a U.S. Geological Survey–New Jersey Geological Survey joint mapping program begun in 1984, calcareous nannofossils were examined from numerous boreholes in southern New Jersey to understand the geologic history of the region. The Clayton borehole (Fig. 1) contained an apparently continuous and fossiliferous sequence across the Paleocene/Eocene boundary, which was discussed in Gibson et al. (1993) and Bybell and Self-Trail (1995). A comparison between the New Jersey coastal plain and Paleocene/Eocene boundary sediments elsewhere in the Atlantic and Gulf coastal plains of the United States is presented in Gibson and Bybell (1995). As part of the New Jersey Coastal Plain Project, Ocean Drilling Program (ODP) Leg 150X, three boreholes were drilled in New Jersey near the ocean margin at Island Beach, Atlantic City, and Cape May. The borehole at Island Beach (Fig. 1) offered the potential for examining sediments of similar age to those in the Clayton borehole but in a more basinward position (Miller et al., 1994). In addition, Deep Sea Drilling Project (DSDP) Site 605, located oceanward of New Jersey (Fig. 1), also contains upper Paleocene and lower Eocene sediments (van Hinte et al., 1987). It was believed that examination of calcareous nannofossils from these three locations would (1) document any upbasin-downbasin variations in calcareous nannofossil distribution patterns, (2) provide additional documentation of calcareous nannofossil occurrences during this time, particularly for the upper part of Zone NP10, which is absent in the Clayton borehole, (3) continue the documentation of calcareous nannofossil evolution, and (4) provide additional clarification for the taxonomy of the genus *Rhomboaster*.

MATERIALS AND METHODS

Calcareous nannofossils were examined from three boreholes that occur in a generally upbasin-downbasin direction from the southern

New Jersey coastal plain to the offshore continental rise (Fig. 1). First is the Clayton borehole, which was drilled in 1988 by the U.S. Geological Survey near the city of Clayton in Gloucester County, New Jersey, in the Pitman East 7.5' quadrangle at 39°39'N, 75°6'W. Second is the Island Beach borehole, which was drilled in 1993 by the U.S. Geological Survey as part of the New Jersey Coastal Plain Drilling Project (ODP Leg 150X) in Ocean County, New Jersey, in the Barnegat Light 7.5' quadrangle at 39°48'N, 74°6'W. The third borehole is DSDP Site 605, which was drilled in 1983 on the upper continental rise ~100 miles southeast of Atlantic City, New Jersey at 38°45'N, 72°37'W.

Calcareous nannofossil samples for all three boreholes were extracted from the central portion of core segment surfaces (freshly broken where possible) at 2- to 3-ft intervals. Clayton borehole samples were collected in the authors' calcareous nannofossil laboratory as soon as coring was completed and core boxes were transported to Reston, VA. Bybell and Self-Trail (1995) presented the calcareous nannofossil data from the late Paleocene and early Eocene portion of the Clayton borehole, and their occurrence chart is reproduced here as Table 1. Calcareous nannofossil samples from the Island Beach borehole were taken by the authors soon after the cores were transported to Rutgers University in Piscataway, New Jersey. Only samples from Martini's (1971) uppermost Paleocene calcareous nannofossil Zone NP9 and lowermost Eocene Zone NP10 were examined from the Island Beach borehole for this study (Table 2). In 1992, Laurel Bybell sampled the uppermost Paleocene and lowermost Eocene portion of the DSDP Site 605 borehole in the DSDP/ODP repository at Lamont-Doherty Earth Observatory in New York. Calcareous nannofossil occurrences from Site 605 are recorded in Table 3.

Calcareous nannofossil slides were prepared using standard setting techniques and were examined with a Zeiss photomicroscope. In addition, samples with the best preservation and highest abundances of calcareous nannofossils were examined with a JEOL 35 scanning electron microscope (SEM). Use of the SEM provided detailed information on the structure of calcareous nannofossil species that is unavailable with a light microscope.

The graphic correlation method was used to compare fossil data from the individual boreholes. The authors followed the technique of Hood (1996) and directly correlated between the individual sections rather than obtaining a standard reference section. This allowed for the opportunity to identify and refine subtle hiatuses between the sec-

¹Miller, K.G., and Snyder, S.W. (Eds.), 1997. *Proc. ODP, Sci. Results*, 150X: College Station, TX (Ocean Drilling Program).

²U.S. Geological Survey, 926 National Center, Reston, VA 20192, U.S.A.
lbybell@usgs.gov

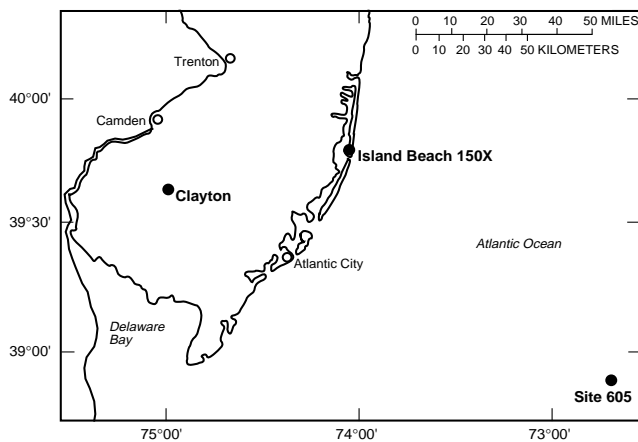


Figure 1. Locations of boreholes (solid circles) that are discussed in text.

tions, to pinpoint reworking of various fossil species, and to identify possible changes in sedimentation rate between the cores.

ZONATION OF THE LATE PALEOCENE AND EARLY EOCENE

In this study, the biostratigraphic zonation of the strata is based primarily upon the calcareous nannofossil zonation of Martini (1971) and secondarily upon the zonation of Bukry (1973, 1978) and Okada and Bukry (1980). The calcareous nannofossil assemblages from the three boreholes typically were sufficient in numbers of specimens, diversity of taxa, and preservational state to allow dating of all samples. However, moving downbasin from Clayton to Island Beach to Site 605, the preservation of calcareous nannofossils decreased significantly through dissolution or recrystallization. There is evidence of reworking in some of the samples, particularly in the Island Beach borehole, and this will be discussed below.

As discussed in Berggren and Aubry (1996), there are five possible positions for the Paleocene/Eocene boundary: (1) the Zone NP9/NP10 calcareous nannofossil boundary, (2) the P5/P6a planktonic foraminiferal boundary, (3) the base of the Ypresian Stage in Belgium, (4) the base of the Harwich Formation in England, and (5) the $\delta^{13}\text{C}$ spike. Until one of these is officially selected, and because this is primarily a calcareous nannofossil investigation, we will continue with the placement of this boundary at the Zone NP9/NP10 boundary, which is defined by the first appearance datum (FAD) of *Rhombaster bramlettei* (Martini, 1971).

Direct comparison of data from this paper with data from elsewhere in New Jersey (Jiang and Wise, 1987; Olsson and Wise, 1987) or at Site 605 (Applegate and Wise, 1987; Lang and Wise, 1987) is complicated somewhat by the fact that they all used the Zone CP8/CP9 boundary of Okada and Bukry (1980) to define the Paleocene/Eocene boundary. Most correlations between the zonation of Martini (1971) and that of Okada and Bukry (1980) place the Zone CP8/CP9 boundary and the Zone NP9/NP10 boundary at the same interval (Okada and Bukry, 1980; Berggren et al., 1985; Perch-Nielsen, 1985). The FADs of both *Rhombaster contortus* and *Discoaster diastypus* define the base of Zone CP9 (Bukry, 1973, 1978). Romein (1979), Perch-Nielsen (1985), Pospichal and Wise (1990), and Bralower and Mutterlose (1995) recognized that the FAD of *R. contortus* occurs above the base of *R. bramlettei*. Lacking reliable occurrences of the species *D. diastypus*, which Pospichal and Wise (1990) and Bralower and Mutterlose (1995) assumed had its FAD near the FAD of *R. bramlettei*, they substituted the FAD of *R. bramlettei* to define the base of Zone CP9. Gibson et al. (1993), Bybell and Self-Trail (1995), and Angori and Monechi (1996) recognized that the FADs of

R. contortus and *D. diastypus* lie well above the FAD of *R. bramlettei*, and they placed the Zone CP8/CP9 boundary within Zone NP10. Data from the current study support this placement. Berggren and Aubry (1996, fig. 13) placed the Zone CP8/CP9 boundary in the lower part of Zone NP10.

The following calcareous nannofossil species are useful in dating upper Paleocene and lower Eocene sediments. The relative positions of FADs and last appearance datums (LADs) are indicated below. Zonal markers for the Martini NP zones are indicated with an *, and a # indicates a zonal marker for the Bukry CP zones. The remaining species have been found by the authors to be biostratigraphically useful, particularly in the Gulf and Atlantic Coastal Plains.

- FAD #**Discoaster lodoensis* = base of Zone NP12, base Zone CP10
- FAD *Discoaster binodosus* = within Zone NP11
- LAD #**Rhombaster contortus* = top of Zone NP10, top Subzone CP9a
- FAD *Rhombaster orthostylus* = upper Zone NP10
- FAD *Rhombaster contortus* = mid- or upper Zone NP10, base Subzone CP9a
- FAD #**Discoaster diastypus* = mid- or upper Zone NP10, base Subzone CP9a
- LAD *Fasciculithus* spp. = lower Zone NP10
- FAD #**Rhombaster bramlettei* = base of Zone NP10
- FAD *Rhombaster spineus* = uppermost Zone NP9
- FAD *Transversopontis pulcher* sensu ampl. = within upper Zone NP9
- FAD *Discoaster mediosus* = within upper Zone NP9
- FAD *Toweius occultatus* = within upper Zone NP9
- FAD #**Campylophaera dela* = within upper Zone NP9, base Subzone CP8b (includes *C. eodela*)
- FAD *Lophodolithus nascens* = within upper Zone NP9
- FAD *Toweius callosus* = within Zone NP9
- FAD *Discoaster lenticularis* = near base of Zone NP9
- FAD #**Discoaster multiradiatus* = base of Zone NP9, base Subzone CP8a

Figure 2 shows calcareous nannofossil species that are biostratigraphically useful in New Jersey and the North Atlantic. It is to be expected that many of these species will prove to be useful in other regions.

RESULTS

Clayton Borehole

Bybell and Self-Trail (1995) examined calcareous nannofossils from 39 samples in the Clayton borehole from 348.5 to 292.0 ft (106.2–89.0 m). Sixteen samples were from the upper Paleocene Vincentown Formation, and 23 samples were from the upper Paleocene and lower Eocene Manasquan Formation (Table 1). The lowest Zone NP9 sediments occur within the Vincentown Formation at 348.5 ft (106.2 m). The lower part of Zone NP9 is presumed to be missing in the Clayton borehole because the lowest Zone NP9 sample at 348.5 ft (106.2 m) contains both *Campylophaera dela* and *Lophodolithus nascens*, which have their FADs in the upper half of Zone NP9 (Perch-Nielsen, 1985). Laurel M. Bybell (unpubl. data) finds that *C. dela* and *L. nascens* are consistently absent from the lower part of Zone NP9 in the Gulf and Atlantic Coastal Plains. This does contrast with a lower position for the FAD of the genus *Campylophaera* found by Bralower and Mutterlose (1995) at ODP Site 865 in the Pacific. A dissolution zone in the Vincentown Formation from 345.2 to 329.0 ft (105.2–100.3 m) has resulted in a notable decrease in calcareous nannofossil and foraminiferal species diversity (Gibson et al., 1993). Similar dissolution intervals have been reported from the upper part of Zone NP9 in many locations: Aubry et al. (1996)

from DSDP Sites 549 and 550, Angori and Monechi (1996) from the Caravaca section in Spain, and Thomas (1996) from Sites 525 and 527. We also find a dissolution interval in the Island Beach borehole (see below). The position of these dissolution intervals may not be consistent with regard to the benthic foraminiferal extinction event, which now appears to have been synchronous around the world (Thomas, 1996), and the Zone NP9/NP10 boundary. It is unclear whether these discrepancies in position of the dissolution interval are real or only apparent due to minor unconformities.

Approximately 10 ft (3 m) above the top of the dissolution zone in the Clayton borehole, between 320.5 and 316.9 ft (97.7 and 96.6 m), there is a gradual lithologic change from the Vincentown Formation to the Manasquan Formation. This 4-ft transition zone corresponds to the worldwide late Paleocene climatic event and contains the benthic foraminiferal extinction, an increase in planktonic foraminifers, a lithologic change from sand to clay, and a change in clay mineral suites from primarily illite/smectite to primarily kaolinite (Gibson et al., 1993). Because of the proximity of the dissolution interval and the climatic event in both the Clayton and Island Beach boreholes, it seems likely that the two events are related.

There may be a short hiatus between the Vincentown and Manasquan Formations, as evidenced by the increase in calcareous nannofossil FADs and LADs to eight species in this interval (Table 1). Farther offshore, a much longer hiatus occurs at this same position in both the Island Beach and Site 605 boreholes (see discussion below).

In the Clayton borehole, the Zone NP9/NP10 boundary, which occurs within the Manasquan Formation between samples at 306.9 and 306.5 ft (93.5 and 93.4 m), represents continuous deposition as can be seen in the graphic correlation presented on Figures 3 and 4. Only 14.5 ft (4.4 m) of lower Zone NP10 are preserved in the Clayton borehole, and these sediments are unconformably overlain by the middle Eocene Shark River Formation at 290 ft (88.4 m; Figs. 3, 4).

There is no evidence for reworking of material in the Clayton borehole. However, several species do appear to be responding to outside environmental controls. The upper range of *Hornibrookina arca* is truncated in the Clayton borehole in comparison to its range in the Island Beach borehole, where it extends above the FAD of *Rhomboaster contortus* (Tables 1, 2; Fig. 3). At Site 605, *H. arca* also has a truncated upper range, and it disappears before the first appearance of *R. contortus* (Table 3). *Hornibrookina arca* is never consistently present in a sedimentary sequence, and, when it is present, it often occurs in large numbers. Paleoenvironmental or paleoecological controls such as water depth, salinity, or temperature may be responsible for the fluctuation in this species' range.

Island Beach Borehole

Thirty-five samples were examined in the Island Beach borehole from 1121.4 to 1018.9 ft (341.8–310.6 m). Eleven samples were from the Vincentown Formation, and 24 samples were from the Manasquan Formation (Table 2). *Discoaster multiradiatus* (FAD defines the base of Zone NP9) first occurs within the Vincentown Formation at 1121.4 ft (341.8 m) in the Island Beach borehole. The authors have observed the co-occurrence of *D. multiradiatus* and *H. riedelii* only in lower Zone NP9 sediments from Virginia, and Bralower and Mutterlose (1995) found a similar distribution at Site 865. *Heliolithus universus* also appears to occur no higher than the lower part of Zone NP9. The lower three Zone NP9 samples from 1121.4 to 1111.8 ft (341.8–338.9 m) can thus be restricted to the lower part of Zone NP9 based on the presence of *D. multiradiatus*, *Heliolithus riedelii*, and *Heliolithus universus*. *Campylosphaera dela* and *Lophodolichus nascens* are absent from this interval. Portions of the upper half of Zone NP9 are present in the Island Beach borehole from 1104.9 to 1077.8 ft (336.8–328.5 m), based on the presence of *Lophodolichus nascens* and *Campylosphaera dela*.

There is a dissolution interval in the Island Beach borehole at the same position in Zone NP9 as in the Clayton borehole (top is ~10 ft

below the Vincentown/Manasquan formational contact), and preservation and diversity of calcareous nannofossil species is noticeably reduced between 1104.9 and 1089.4 ft (336.8 and 332.0 m; Table 2).

As in the Clayton borehole, at Island Beach there is a lithologic change at the Vincentown/Manasquan contact (1076 ft [371 m]) from clay below to silty clay above the contact, and the contact is disconformable between the two formations (Miller et al., 1994). The lower part of the Manasquan Formation (uppermost part of Zone NP9 in the Clayton borehole) is missing in the Island Beach borehole (Figs. 3, 5), and the basal Manasquan sample at 1075.8 ft (327.9 m) is in Zone NP10. As a result, there are no sediments at Island Beach that are equivalent to the lowest Manasquan Formation in the Clayton borehole (319.4–306.9 ft [97.4–93.5 m]; Table 1). As confirmed by Aubry et al. (1996), the authors have long recognized the abundance of minor unconformities in marine sedimentary sequences, both in the nearshore and offshore regimes. These previously unrecognized unconformities are now being identified because of recent studies using closely spaced sampling intervals combined with a large number of documented calcareous nannofossil FADs and LADs.

There is reworking of Vincentown material up into much of the Manasquan Formation at Island Beach, and this is most noticeable in the interval from the basal Manasquan sample at 1075.8 ft (327.9 m) up to 1059.9 ft (323.1 m). Pak et al., Chapter 23, this volume, find evidence for reworking of benthic foraminifers within this interval (1075–1065 ft [327.7–324.6 m]). Five calcareous nannofossil species—*Biantholithus astralis*, *Fasciculithus alanii*, *Fasciculithus schaubii*, *Scapholithus apertus*, and *Toweius eminens* var. *tovae*, which have their LADs in the upper part of Zone NP9 (Bybell and Self-Trail, 1995)—are reworked into Zone NP10 in the lower part of the Manasquan Formation in the Island Beach borehole (Table 2; Figs. 3, 5). Bralower and Mutterlose (1995) also found *F. alanii* to be absent from Zone NP10, as well as *F. schaubii*, except for a rare occurrence in the lowest Zone NP10 in Core 865C. The continuance of large numbers of *Toweius eminens* var. *eminens* into Zone NP10 in the Island Beach borehole and at Site 605, when it occurs no higher than Zone NP9 in the Clayton borehole, is believed to be the result of paleoecological or paleoenvironmental preferences for this species, rather than reworking.

Whereas the Clayton borehole only had 14.5 ft (4.4 m) of Zone NP10 sediments, the Island Beach borehole has 57 ft (17.4 m) of Zone NP10 sediments, and both the lower and upper parts of the zone are represented. However, most of the Island Beach borehole is what normally would be considered to be the lower part of Zone NP10 because *Rhomboaster contortus* (FAD in upper half of Zone NP10) is only present in the upper two Zone NP10 samples at 1020.9 ft (311.2 m) and 1018.9 ft (310.6 m), and *Rhomboaster orthostylus* is only present in the uppermost Zone NP10 sample at 1018.9 ft (310.6 m). A sample from 1016.9 ft (310.0 m) is in Zone NP11. A similar placement for the FADs of *R. contortus* and *R. orthostylus* occurs at Site 605 (see below). Angori and Monechi (1996) reported the FAD of *R. contortus* near the middle of Zone NP10 at Caravaca, as did Wei and Zhong (1996) and Aubry et al. (1996) at DSDP Site 550. However, at DSDP Site 690B, the FADs of *R. contortus* and *R. orthostylus* occur much nearer the top of Zone NP10 in what is presumed to be a discontinuous section (Aubry et al., 1996; Wei and Zhong, 1996). If the FADs of *R. contortus* and *R. orthostylus* actually do occur in the middle of Zone NP10, then there must be an unconformity at Island Beach that represents some of upper Zone NP10. Such a hiatus, however, was not detected using graphic correlation (Fig. 5).

DSDP Site 605 Borehole

Lang and Wise (1987) examined 9 samples from Zone NP9 at Site 605 from 1973.4 to 1835.6 ft (601.5–559.5 m), and Applegate and Wise (1987) examined 2 samples from Zone NP9 at Site 605 from 1855.3 to 1835.6 ft (565.5–559.5 m) and 5 samples from Zone NP10 from 1830.7 to 1809.0 ft (558.0–551.4 m).

Table 1 (continued).

Age	Zone	Formation	Depth (ft)	Abundance Preservation	<i>M. inversus</i>	<i>Neochiastocyclus concinnus</i> s. ampl.	<i>N. sp. cf. N. imbrici</i>	<i>Neococcolithes dabius</i>	<i>N. spp. aff. N. protenus</i>	<i>Neorepidolithus</i> spp.	<i>Platocyclus signoides</i>	<i>Pontosphaera</i> spp.	<i>Rhombaster bramlettei</i>	<i>R. spinus</i>	<i>Scapholithus apertus</i>	<i>Sphenolithus primus</i>	<i>Thoracosphaera</i> spp.	<i>Toweius callosus</i>	<i>T. emimens</i> var. <i>emimens</i>	<i>T. emimens</i> var. <i>tovae</i>	<i>T. occultatus</i>	<i>T. pertusus</i>	<i>T. serotinus</i>	<i>Transversopontis pulcher</i>	<i>Zygodiscus herlyni</i>	<i>Zyghabolithus bijugatus</i>		
early Eocene	NP 10		292.0	C F	X X					X	X				X X					X X X X								
			294.5	F P	X X							X				X					X X X X							
			296.5	C F	X X							X	X			X X X					X X X X							
			298.5	C G	X X				X		X	X X				X X X					X X X X					X		
			300.5	C F	X X X	X					X	X X X				X X X					X X X X X					X X		
			302.5	C F	X X X	X					X	X X X X				X X X					X X X X					X X		
			306.5	C F	X X X X	X					X	X X X				X X X					X X X X					X X		
			late Paleocene	NP 9	Manasquan Formation	306.9	C F	X X				X	X				X	X X X					X X X X				X X	
307.2	C G	X X X				X				X	X				X	X X					X X X X				X X			
307.9	C F	X X X				X					X				X	1	X				X X X X				X X			
308.3	C F	X X X				X					X						X				X X X X				X X			
308.7	C F	X X				X					X						X				X X X X				X X			
309.0	C F	X X				X					X X	X				X	X				X X X X				X X			
309.6	C G	X X X				X					X X	X				X	X				X X X X				X X			
310.3	C F	X X X				X					X					X	X X				X X X X				X X			
310.8	C F	X X X				X					X						X				X X X X				X X			
311.0	C F	X X X				X					X						X X				X X X X				X X			
313.3	C F	X X X				X					X						X				X X X X				X X			
314.0	A F	X X				X					X X	X					X X				X X X X				X X			
317.0	C F	X X X				X					X X	X					X X				X X X X				X X			
317.4	C F	X X X				X					X X	X					X X X				X X X X				X X			
318.5	C F	X				X					X	X					X X				X X X X				X X			
319.4	F F	X		X					X						X	X			X X X X				X X					
321.4	A F	X		X					X X	X X					X X X X				X X X X				X X					
322.0	C F	X X		X					X X	X X					X X	X X			X X X X				X X					
324.1	C P														X				X X X				X X					
324.4	C F	X X							X X	X X					X	X X			X X X				X X					
327.0	F P	X														X X X			X X X				X X					
329.0	F P																											
331.0	C P	X																		X	X							
334.0	F P	X																		X								
335.5	F P																											
337.0	F P																			X								
339.0	F P																											
342.0	F P	X														X	X X			X								
344.0	F P	X															X X			X								
345.2	F P																X X			X X								
347.0	F P	X X	X					X X	X X						X X	X X			X X	X				X X				
348.5	C F	X X X	X					X	X					X X X X	X X X				X X	X				X				

Paleocene/Eocene boundary at 1850.0 ft (563.9 m) or almost exactly where we place the boundary. Photographs of the Site 605 core at this interval (van Hinte et al., 1987, p. 401) show a lithologic change at this same depth (1850.0 ft or 563.9 m). Olsson and Wise (1987) also placed the Paleocene/Eocene boundary at this same lithologic contact at Site 605, which is the downdip facies equivalent of the Vincentown/Manasquan formational boundary.

There is no evidence of reworking of Zone NP9 sediments into Zone NP10 at Site 605, as was found in the Island Beach borehole, and lower Zone NP10 calcareous nannofossil occurrences at Site 605 and in the Clayton borehole are quite similar (Tables 1 and 3). Site 605 has 43 ft (13.1 m) of Zone NP10 sediments, Island Beach has 57 ft (17.4 m), and the Clayton borehole only has 14.5 ft (4.4 m). Both *Rhombaster contortus* and *R. orthostylus* occur in Zone NP10 sediments at Site 605, but as in the Island Beach borehole, they are only in the very upper part of this zone, which may be indicative of a small unconformity. *Rhombaster contortus*, for example, is confined to the upper 12 ft (3.7 m), and *R. orthostylus* is only present in the upper 2 ft (0.6 m) of Zone NP10.

DISCUSSION

Onshore/Offshore Patterns

One goal of this study was to document upbasin-downbasin variations in calcareous nannofossil distribution patterns. During the late Paleocene and early Eocene, sediments at Clayton (the farthest upbasin position) were being deposited in middle neritic depths (T.G. Gibson, pers. comm., 1996) with deepening of waters offshore to lower bathyal at Site 605 (E. Thomas, pers. comm., 1996). At the Clayton borehole (farthest upbasin position), the base of Zone NP10 occurs at ~190 ft (58 m) below sea level. Downdip at Island Beach, the base of Zone NP10 occurs at 1064 ft (324 m) below sea level, and at Site 605 it is at 9048 ft (2758 m) below sea level. The base of Zone NP10 drops 874 ft (266 m) from Clayton to Island Beach in a 20-mile downbasin transect or ~44 ft per mile. Between Island Beach and Site 605, the base of Zone NP10 drops 7984 ft (2434 m) in a 110-mile downbasin transect or 73 ft per mile. However, it is unlikely that these elevations for the base of Zone NP10 reflect relative positions

Table 3 (continued).

Age	Zone	Core, section, interval (cm)	Depth (mbsf)	Depth (ftbsf)	Abundance Preservation																						
Paleocene	NP 9	44-6, 15	565.1	1854.0	A F																						
		44-6, 30	565.3	1854.6	A F																						
		44-6, 74	565.7	1855.9	A F																						
		44-6, 89	565.9	1856.6	A F																						
		44-6, 122	566.2	1857.6	A F																						
		45-1, 25	567.3	1861.2	A F																						
		45-1, 32	567.4	1861.5	A F																						
		45-1, 98	568.1	1863.8	A G																						
		45-1, 112	568.2	1864.2	A F																						
		45-2, 25	568.8	1866.1	A F																						
		45-2, 112	569.7	1869.1	A F																						
		45-3, 87	571.0	1873.3	A F																						
		45-4, 71	572.3	1877.6	A G																						
		45-5, 86	574.0	1883.2	A G																						
		45-6, 32	574.9	1886.1	A F																						
		46-1, 80	577.5	1894.7	A G																						

Age	Zone	Core, section, interval (cm)	Depth (mbsf)	Depth (ftbsf)	Abundance Preservation																						
Paleocene	NP 9	44-6, 15	565.1	1854.0	A F																						
		44-6, 30	565.3	1854.6	A F	X																					
		44-6, 74	565.7	1855.9	A F																						
		44-6, 89	565.9	1856.6	A F	X																					
		44-6, 122	566.2	1857.6	A F	X																					
		45-1, 25	567.3	1861.2	A F																						
		45-1, 32	567.4	1861.5	A F	X																					
		45-1, 98	568.1	1863.8	A G																						
		45-1, 112	568.2	1864.2	A F	X																					
		45-2, 25	568.8	1866.1	A F																						
		45-2, 112	569.7	1869.1	A F																						
		45-3, 87	571.0	1873.3	A F	X																					
		45-4, 71	572.3	1877.6	A G	X																					
		45-5, 86	574.0	1883.2	A G	X																					
		45-6, 32	574.9	1886.1	A F	X																					
		46-1, 80	577.5	1894.7	A G	X																					

are on a line that is oblique and inverse to the plane of symmetry of the rhombohedron.” The current authors disagree with these structural differences as a viable way to separate *R. cuspis* from *T. bramlettei* because they only represent two different views of the same species. Figure 6 illustrates a clay model from two different views: view A corresponds to Aubry’s (1996) figure 2a, which she would call *T. bramlettei*, and view B (same specimen tilted forward 30°) corresponds to Aubry’s figure 2c, which she would call *R. cuspis*. *Rhomboaster cuspis* and *T. bramlettei* have exactly the same structure and are properly placed in one species, *R. bramlettei*.

The current authors propose that the clay model representation of *T. bramlettei* on figure 5-1e, 2e, 3e of Wei and Zhong (1996), which has all six ray terminations in the same plane, does not correspond to any known fossil specimens, and even their scanning electron photomicrographs of *T. bramlettei* on figure 4, specimens 3–4,6 clearly show that the ray terminations are not in the same plane. There is no doubt that longer rayed forms do appear to be flatter than shorter rayed forms. However, as stated by Bybell and Self-Trail (1995), “a clay model of *R. cuspis* with very short arms was turned into a model of *R. bramlettei* merely by lengthening the rays. As the rays were lengthened, in order to maintain symmetry within a specimen, the an-

gles on each face of the rhombohedron were forced to change: the angle increased on the corner without a ray” (the β angle of Wei and Zhong, 1996), “and the angles decreased on the three corners containing rays.” However, Wei and Zhong used the β angle to differentiate *Rhomboaster cuspis* from *Tribrachiatus bramlettei*, and they stated that “specimens with angle β < 130° look convex and thick and were recorded as *Rhomboaster*; those with angle β > 130° appear relatively flat and were recorded as *T. bramlettei*.” But their long-rayed specimen on figure 5-1d, 2d, 3d, which they placed in *R. cuspis*, has a β angle of more than 130°. The current authors believe that use of the β angle is a misleading and inaccurate measurement because the size of the angle can appear to vary significantly just by viewing the specimen from slightly different positions and with different ray lengths. The simplest and easiest solution is not to separate *R. cuspis* and *T. bramlettei*.

The Clayton borehole contained only the lower part of Zone NP10, but Island Beach, Site 605, Site 550, and Caravaca also contain material from the upper part of Zone NP10. Extensive examination of both lower and upper Zone NP10 material confirmed that *R. bramlettei* does not change its basic shape within Zone NP10 by flattening. Specimens from Plate 1, Figures 3, 6–8 are all from the upper

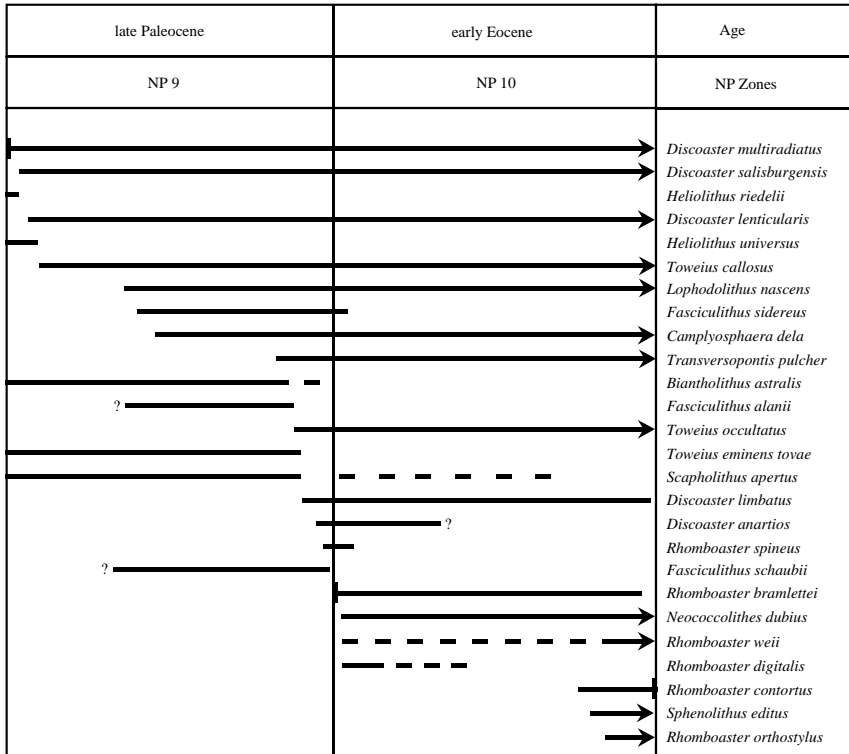


Figure 2. Stratigraphically useful calcareous nannofossil species in Zones NP9 and NP10 in New Jersey and the offshore Atlantic Ocean. A question mark indicates an unknown termination for a species' range, a dashed horizontal line indicates sporadic occurrence, and an arrow indicates that the range extends into Zone NP11. A horizontal line with a vertical end bar represents the occurrence of Martini's (1971) zonal marker species. (Author correction: *Toweius eminens tovae* should be *Toweius eminens* var. *tovae*.)

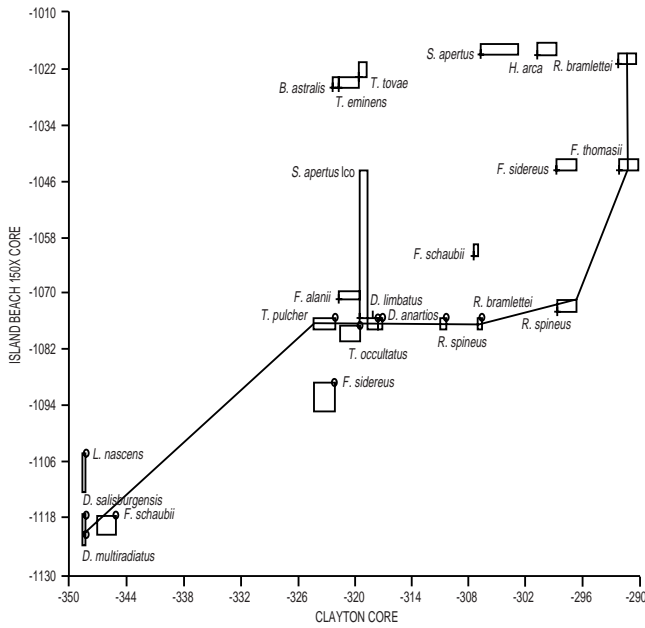


Figure 3. Graphic correlation plot of the Island Beach 150X borehole and the Clayton borehole, New Jersey. For Figures 3, 4, and 5, stratigraphic up is to the top and to the right. First occurrence events are plotted as "o" with the sample-interval boxes extended down and to the left; last occurrence events are plotted as "+" with the sample-interval boxes extended up and to the right.

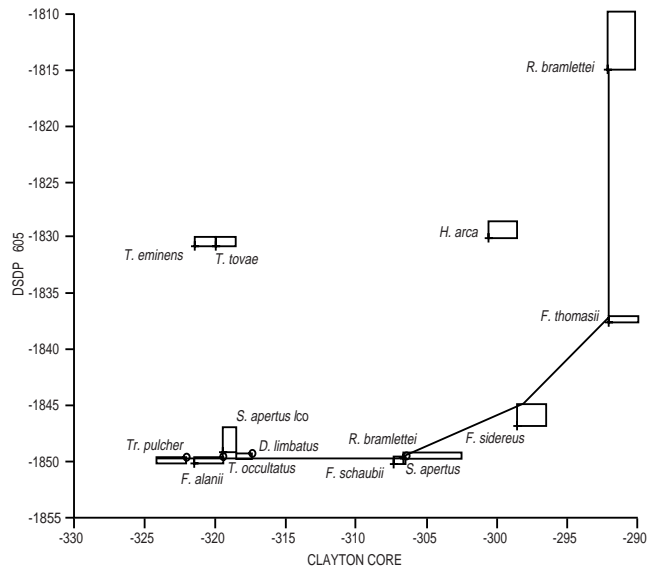


Figure 4. Graphic correlation plot of the Clayton borehole, New Jersey, and the DSDP Site 605 borehole, Atlantic Ocean. See Figure 3 caption for explanation of symbols.

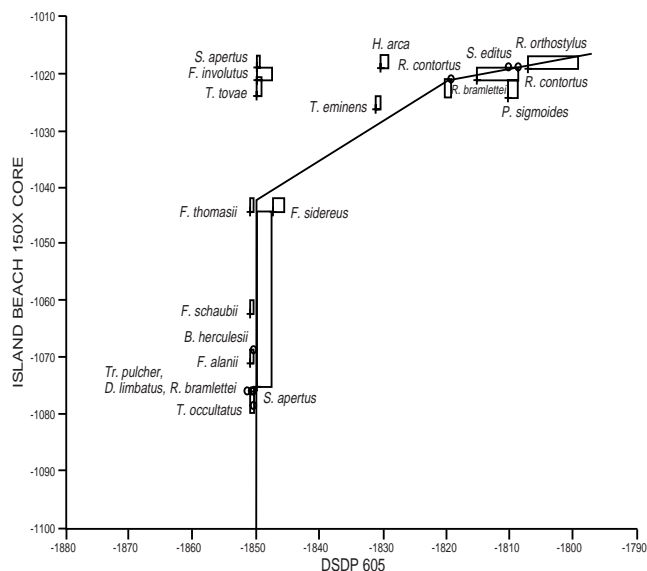


Figure 5. Graphic correlation plot of the Island Beach 150X borehole, New Jersey, and the DSDP Site 605 borehole, Atlantic Ocean. See Figure 3 for explanation of symbols.

part of Zone NP10, and they are indistinguishable from lower Zone NP10 specimens that were illustrated by Bybell and Self-Trail (1995) on plates 22 and 23.

SYSTEMATIC PALEONTOLOGY

Genus *BLACKITES*

Blackites herculesii (Stradner, 1969) Bybell & Self-Trail, n. comb.
(Pl. 5, Figs. 3–6)

Rhabdosphaera herculea Stradner, 1969, p. 415, pl. 89, figs. 9–12.

Remarks: The SEM photomicrograph on Plate 5, Figure 4 clearly shows the presence of three cycles on the basal plate, which conforms to the description of the genus *Blackites* as emended by Stradner in Stradner and Edwards (1968). Stradner (1969, p. 415) stated that the derivation of the name was “Hercules = name of hero (Greek Mythology).” Therefore, *herculea* has been changed to *herculesii* according to the rules of the International Code of Botanical Nomenclature (Greuter, 1988, 1994, Recommendation 23A), which was discussed in van Heck (1990, p. 20).

Occurrence: *Blackites herculesii* only occurs in the early Eocene Zone NP10 in the Island Beach borehole, New Jersey and in the DSDP Site 605 borehole.

Genus *ELLIPSOLITHUS*

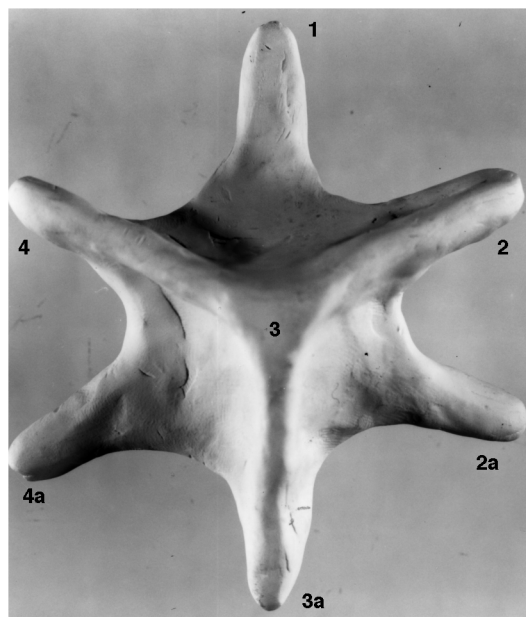
Ellipsolithus sp.
(Pl. 4, Figs. 3–5)

Remarks: *Ellipsolithus* sp., which contains numerous small perforations in the central area, also has been observed by Aubry (pers. comm., 1996), who will publish a description of this species. In the light microscope, it can be difficult to distinguish between *Ellipsolithus* sp. and *Ellipsolithus distichus* in poorly preserved material, particularly if there is extensive recrystallization, which fills in most or all of the perforations in *E. distichus*. However, *Ellipsolithus* sp. has at least one additional ring of perforations in the central area and frequently has a wider central region than *E. distichus*.

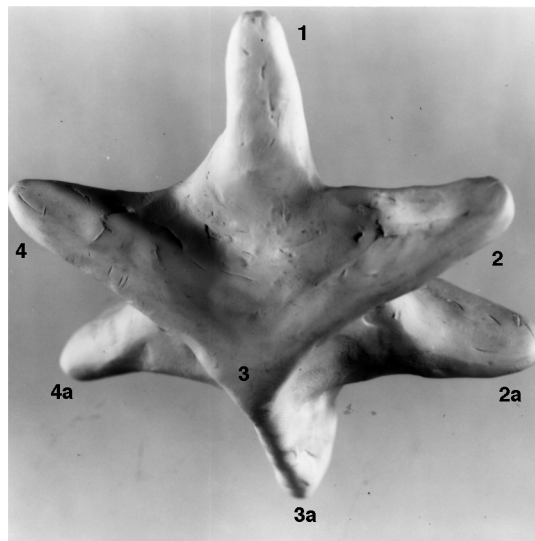
Occurrence: *Ellipsolithus* sp. was observed in Zone NP10 in the Island Beach borehole and probably in Zones NP10–12 in the DSDP Site 605 borehole where poor preservation made recognition of this species difficult.

Genus *RHOMBOASTER*

Rhomboaster digitalis (Aubry, 1996) Bybell & Self-Trail n. comb.
(Pl. 2, Figs. 3–7)



A



B

Figure 6. Clay model of *Rhomboaster bramlettei*, showing two different views of same specimen. View A corresponds to *Tribrachiatius bramlettei* of Aubry (1996, fig. 2-a), which she reproduced from Romein (1979, p. 193), and view B corresponds to *Rhomboaster cuspidis* of Aubry (1996, fig. 2-c), which she reproduced from Romein (1979, p. 190). Numbers on the figure correspond to those in Aubry (1996) and Romein (1979).

Tribrachiatius digitalis Aubry, 1996, p. 245, pl. 1, figs. 1–12; pl. 2, figs. 11–12

Remarks: The original illustrations of this species were confined to light micrographs. Scanning electron micrographs now are provided for this species (Plate 2, figs. 3–7). *Tribrachiatius digitalis* is herein changed to *Rhomboaster digitalis* because its structure is similar to other members of this genus. This combination was suggested but not officially proposed by Angori and Monechi (1996). In heavily overgrown specimens it can be difficult to distinguish the flat ray terminations of *R. digitalis* from the offset terminations of *Rhomboaster contortus*.

It is possible that *Rhomboaster digitalis* evolved into *R. contortus*, which it most closely resembles and predates, by torquing of each ray. However, the

ranges of *R. digitalis* and *R. contortus* do not appear to overlap, and no intermediary specimens have been observed. Wei and Zhong (1996) proposed that *R. bramlettei* evolved into *R. contortus* by flattening and shifting of the rays. Both scenarios cannot be correct, and additional studies of closely spaced samples are necessary to resolve this issue.

Occurrence: *Rhomboaster digitalis* occurs in the lower part of Zone NP10 in the Island Beach borehole (Table 2). Aubry (1996) reported it from DSDP Sites 117 and 550, the Owaina-Gurnah section in Egypt, and the Island Beach borehole. This short-ranging species is absent at Clayton and Site 605, and this may be due to a small unconformity encompassing this part of the section.

Rhomboaster weii Bybell & Self-Trail n. sp.
(Pl. 3, Figs. 5–9)

Diagnosis: A robust member of the genus *Rhomboaster* with triradiate arms that terminate bluntly at an equal distance from the central area. This species is named in honor of Wuchang Wei.

Description: A triradiate calcareous nannofossil consisting of three thick and somewhat rectangular rays that are bluntly truncated and with no conspicuous terminal notch or bifurcation. The angle between each ray is equal, resulting in *R. weii* having a highly symmetrical appearance. Specimens of *R. weii* exhibit a slight thickening of the central area which becomes more pronounced in specimens that are somewhat overgrown. The diameter of *R. weii* ranges from 5 to 8 μm .

Remarks: *Rhomboaster weii* most closely resembles *Rhomboaster orthostylus*, which also has three rays. However, *R. weii* can be differentiated from *R. orthostylus* by its thicker and more truncated rays, its lack of terminal bifurcation, and its broad, thickened central area. *Rhomboaster weii* typically is somewhat smaller than *R. orthostylus* and has its first appearance datum in lower Zone NP10, well before the first appearance of *R. contortus* or *R. orthostylus*. *Rhomboaster weii* is easily identified from scanning electron photomicrographs, but it is more difficult to distinguish from heavily overgrown specimens of *R. orthostylus* in the light microscope. It is unclear where *R. weii* fits in the genus *Rhomboaster* lineage.

Holotype: Plate 3, Figure 5, SEM photomicrograph number 510–6.

Paratype: Plate 3, Figure 6, SEM photomicrograph number 530–5.

Type Locality: Holotype, New Jersey, Island Beach borehole 150X, 1016.9 ft, Zone NP11, Manasquan Formation. Paratype, New Jersey, Island Beach borehole 150X, 1073.9 ft, Zone NP10, Manasquan Formation.

Occurrence: This species occurs in lower Zone NP10 and lower Zone NP11 in New Jersey and in Alabama. *Rhomboaster weii* is never very common, and it is quite possible that its range extends beyond what is recorded here.

Depository: The original scanning electron photomicrographs and negatives are stored at the U.S. Geological Survey in Reston, VA.

SUMMARY

Examination of closely spaced samples from all three sites made it possible to document significant differences in the ages of preserved sediments from borehole to borehole and to document changes in floral abundances from an upbasin/downbasin perspective. These differences, combined with biostratigraphic information from other boreholes in the New Jersey coastal plain, reveal a complex mosaic of sediments in this region. For example, in the Clayton borehole, the lower part of Zone NP9 is missing, whereas it is present at Island Beach. The Clayton borehole contains the uppermost part of Zone NP9, but sediments of this age are missing at both Island Beach and Site 605. The lowest part of Zone NP10 appears to be present at all three locations. The upper part of Zone NP10 is missing in the Clayton borehole but is present at Island Beach and the Site 605 borehole.

There is evidence that the distribution of *Hornibrookina arca* and *Toweius emineus* var. *emineus* may be controlled by paleoenvironmental conditions, although the nature of these conditions is unknown. In the Clayton borehole, the most updip (upbasin) of the three, *T. emineus* var. *emineus* has its last appearance at an earlier date than the two downdip (downbasin) boreholes, possibly indicating a deeper water preference for this species.

In the study area, braarudosphaerids have higher abundances in deeper water than in shallower water, and significantly higher abundances in Zone NP10 than in Zone NP9. Neither preservation nor water depth appear to be controlling factors. This unexpected distribution offers only additional puzzlement to the already confusing distribution of this group. The distribution of *Zygrhablithus bijugatus* parallels that of the braarudosphaerids.

Discoaster multiradiatus appears to evolve into *Discoaster bardiensis*, and *Sphenolithus anarrhopus* appears to evolve into *Sphenolithus radians*.

Through examination of many specimens, it is confirmed that *Rhomboaster cuspis* is indeed a junior synonym of *Tribrachiatius bramlettei*, and the proper name is *Rhomboaster bramlettei*. *Tribrachiatius digitalis* is changed to *Rhomboaster digitalis*, the new species *Rhomboaster weii* is established, and *Rhabdosphaera herculea* is changed to *Blackites herculesii*.

ACKNOWLEDGMENTS

We wish to thank James J. Pospichal of Hamilton College and Timothy J. Bralower of the University of North Carolina for their thoughtful reviews of this paper. We wish to dedicate this paper to James P. Owens, who spent many years studying the geology of New Jersey. For his many insights and undaunted enthusiasm, we are forever indebted to him. This paper was written as part of the International Geological Correlation Programme (IGCP) Project 308.

REFERENCES

- Angori, E., and Monechi, S., 1996. High-resolution calcareous nannofossil biostratigraphy across the Paleocene/Eocene boundary at Caravaca (southern Spain). *Israel J. Earth Sci.*, 44:197–206.
- Applegate, J.L., and Wise, S.W., Jr., 1987. Eocene calcareous nannofossils, Deep Sea Drilling Project Site 605, upper continental rise off New Jersey U.S.A. In van Hinte, J.E., Wise, S.W., Jr., et al., *Init. Repts. DSDP*, 93: Washington (U.S. Govt. Printing Office), 685–698.
- Aubry, M.-P., 1996. Towards an upper Paleocene-lower Eocene high resolution stratigraphy based on calcareous nannofossil stratigraphy. *Israel J. Earth Sci.*, 44:239–253.
- Aubry, M.-P., Berggren, W.A., Stott, L., and Sinha, A., 1996. The upper Paleocene-lower Eocene stratigraphic record and the Paleocene/Eocene boundary carbon isotope excursion: implications for geochronology. In Knox, R.W.O'B., Corfield, R.M., and Dunay, R.E. (Eds.), *Correlation of the Early Paleogene in Northwestern Europe*, Spec. Publ.—Geo. Soc. Am., 101:353–380.
- Berggren, W.A., and Aubry, M.-P., 1996. A late Paleocene-early Eocene NW European and North Sea magnetobiochronological correlation network. In Knox, R.W.O'B., Corfield, R.M., and Dunay, R.E. (Eds.), *Correlation of the Early Paleogene in Northwest Europe*, Spec. Publ.—Geo. Soc. Am., 101:309–352.
- Berggren, W.A., Kent, D.V., Flynn, J.J., and van Couvering, J.A., 1985. Cenozoic geochronology. *Geol. Soc. Am. Bull.*, 96:1407–1418.
- Bralower, T.J., and Mutterlose, J., 1995. Calcareous nannofossil biostratigraphy of Site 865, Allison Guyot, Central Pacific Ocean: a tropical Paleogene reference section. In Winterer, E.L., Sager, W.W., Firth, J.V., and Sinton, J.M. (Eds.), *Proc. ODP, Sci. Results*, 143: College Station, TX (Ocean Drilling Program), 31–74.
- Bramlette, M.N., and Riedel, W.R., 1954. Stratigraphic value of discoasters and some other microfossils related to Recent coccolithophores. *J. Paleontol.*, 28:385–403.
- Bramlette, M.N., and Sullivan, F.R., 1961. Coccolithophorids and related nannoplankton of the early Tertiary in California. *Micropaleontology*, 7:129–188.
- Brönnimann, P., and Stradner, H., 1960. Die Foraminiferen- und Discoasterzonen von Kuba und ihre interkontinentale Korrelation. *Erdoel-Zeit.*, 76:364–369.
- Bukry, D., 1971. Cenozoic calcareous nannofossils from the Pacific Ocean. *Trans. San Diego Soc. Nat. Hist.*, 16:303–327.

- , 1973. Low-latitude coccolith biostratigraphic zonation. In Edgar, N.T., Saunders, J.B., et al., *Init. Repts. DSDP*, 15: Washington (U.S. Govt. Printing Office), 685–703.
- , 1978. Biostratigraphy of Cenozoic marine sediment by calcareous nannofossils. *Micropaleontology*, 24:44–60.
- Bybell, L.M., and Gartner, S., 1972. Provincialism among mid-Eocene calcareous nannofossils. *Micropaleontology*, 18:319–336.
- Bybell, L.M., and Self-Trail, J.M., 1995. Evolutionary, biostratigraphic, and taxonomic study of calcareous nannofossils from a continuous Paleocene/Eocene boundary section in New Jersey. *Geol. Surv. Prof. Pap. U.S.*, 1554.
- Faris, M., 1992. Morphometry of *Discoaster multiradiatus* Bramlette & Riedel (1954) and its biochronological significance in the early Paleogene of Egypt. *Delta J. Sci.*, 16:152–170.
- Gibson, T.G., and Bybell, L.M., 1995. Sedimentary patterns across the Paleocene/Eocene boundary in the Atlantic and Gulf Coastal Plains of the United States. *Geologie*, 103:237–265.
- Gibson, T.G., Bybell, L.M., and Owens, J.P., 1993. Latest Paleocene lithologic and biotic events in neritic deposits of southwestern New Jersey. *Paleoceanography*, 8:495–514.
- Greuter, W., 1988. *International Code of Botanical Nomenclature*. Königstein (Koeltz Scientific Books), 1–328.
- , 1994. *International Code of Botanical Nomenclature*. Königstein (Koeltz Scientific Books), 1–389.
- Hood, K.C., 1996. Evaluating the use of average composite sections and derived correlations in the graphic correlation technique. In Mann, K.O., and Lane, H.R., (Eds.), *Graphic Correlation: Spec. Publ.—Soc. Econ. Petrol. Mineral.*, 53:83–93.
- Jiang, Y.W., and Wise, S.W., 1987. Paleocene-Eocene calcareous nannofossils of onshore wells from the coastal plain of New Jersey and Maryland, U.S.A. In van Hinte, J.E., Wise, S.W., Jr., et al., *Init. Repts. DSDP*, 93: Washington (U.S. Govt. Printing Office), 699–711.
- Lang, T.H., and Wise, S.W., Jr., 1987. Neogene and Paleocene-Maestrichtian calcareous nannofossil stratigraphy, Deep Sea Drilling Project Sites 604 and 605, Upper Continental Rise off New Jersey: sedimentation rates, hiatuses, and correlations with seismic stratigraphy. In van Hinte, J.E., Wise, S.W., Jr., et al., *Init. Repts. DSDP*, 93: Washington (U.S. Govt. Printing Office), 661–683.
- Martini, E., 1971. Standard Tertiary and Quaternary calcareous nannoplankton zonation. In Farinacci, A. (Ed.), *Proc. 2nd Int. Conf. Planktonic Microfossils Roma*: Rome (Ed. Tecnosci.), 2:739–785.
- Miller, K.G., Sugarman, P., Van Fossen, M., Liu, C., Browning, J.V., Queen, D., Aubry, M.-P., Burckle, L.D., Goss, M., and Bukry, D., 1994. Island Beach site report. In Miller, K.G., et al., *Proc. ODP, Init. Repts.*, 150X: College Station, TX (Ocean Drilling Program), 5–33.
- Okada, H., and Bukry, D., 1980. Supplementary modification and introduction of code numbers to the low-latitude coccolith biostratigraphic zonation (Bukry, 1973; 1975). *Mar. Micropaleontol.*, 5:321–325.
- Olsson, R.K., and Wise, S.W., 1987. Upper Maestrichtian to middle Eocene stratigraphy of the New Jersey slope and coastal plain. In van Hinte, J.E., Wise, S.W., Jr., et al., *Init. Repts. DSDP*, 93 (Pt. 2): Washington (U.S. Govt. Printing Office), 1343–1365.
- Perch-Nielsen, K., 1985. Cenozoic calcareous nannofossils. In Bolli, H.M., Saunders, J.B., and Perch-Nielsen, K. (Eds.), *Plankton Stratigraphy*: Cambridge (Cambridge Univ. Press), 427–554.
- Pospichal, J.J., and Wise, S.W., Jr., 1990. Paleocene to middle Eocene calcareous nannofossils of ODP Sites 689 and 690, Maud Rise, Weddell Sea. In Barker, P.F., Kennett, J.P., et al., *Proc. ODP. Sci. Results*, 113: College Station, TX (Ocean Drilling Program), 613–638.
- Romein, A.J.T., 1979. Lineages in early Paleogene calcareous nannoplankton. *Utrecht Micropaleontol. Bull.*, 22:1–231.
- Shamrai, I.A., 1963. Nekotorye formy verkhnemelovykh i paleogenovykh kokkolitov i diskoasterov na yuge russkoi platformy. *Izv. Vyssh. Ucheb. Zaved. Geol. i Razy.*, 6:27–40.
- Siesser, W.G., Bralower, T.J., and De Carlo, E.H., 1992. Mid-Tertiary *Braarudosphaera*-rich sediments on the Exmouth Plateau. In von Rad, U., Haq, B.U., et al., *Proc. ODP, Sci. Results*, 122: College Station, TX (Ocean Drilling Program), 653–663.
- Stradner, H., 1969. The nannofossils of the Eocene flysch in the Hagenbach Valley (northern Vienna Woods), Austria. *Annal. Soc. Geol. Pologne*, 39:403–432.
- Stradner, H., and Edwards, A.R., 1968. Electron microscopic studies on upper Eocene coccoliths from the Oamaru diatomite, New Zealand. *Jahrb. Geol. Bundesanst. (Austria)*, 13:1–66.
- Tan Sin Hok, 1927. *Discoasteridae incertae sedis*. *Koninkl. Nederlandse Akad. Wetenschap. Proc. Sect. Sci.*, 30:411–419.
- Thomas, E., 1996. The Paleocene-Eocene benthic foraminiferal extinction and stable isotope anomalies. In Knox, R.W. O'B., Corfield, R.M., and Dunary, R.E. (Eds.), *Correlation of the Early Paleogene in Northwest Europe*, Spec. Publ.—Geol. Soc. Am., 101:401–441.
- van Heck, S.E., 1990. The ICBN: things you need to know: 1. *Int. Nannoplankton Assoc. Newslet.*, 12:19–20.
- van Hinte, J., Wise, S.W., and Leg 93 Shipboard Party. 1987. Sites 604 and 605. In van Hinte, J.E., Wise, S.W., Jr., et al., *Init. Repts. DSDP*, 93: Washington (U.S. Govt. Printing Office), 277–413.
- Wei, W., 1992. Biometric study of *Discoaster multiradiatus* and its biochronological utility. *Mem. Sci. Geol.*, 32:219–235.
- Wei, W., and Zhong, S., 1996. Taxonomy and magnetobiochronology of *Tribrachiatus* and *Rhomboaster*; two genera of calcareous nannofossils. *J. Paleontol.*, 70:7–22.

Date of initial receipt: 18 March 1996

Date of acceptance: 16 September 1996

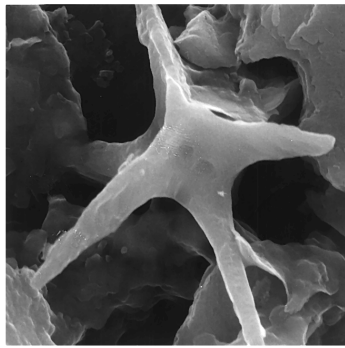
Ms 150XSR-307

APPENDIX

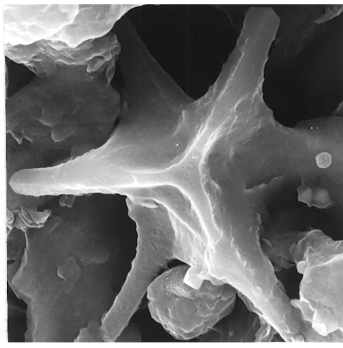
Calcareous Nannofossil Species Considered in this Report

(In alphabetical order of generic epithets)

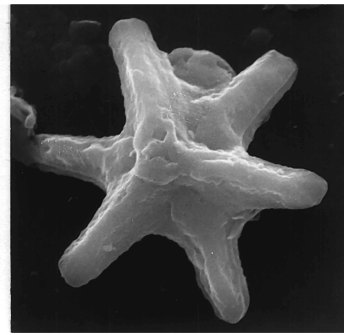
- Biantholithus astralis* Steinmetz & Stradner, 1984
Biantholithus sparsus Bramlette & Martini, 1964
Blackites herculesii (Stradner, 1969) Bybell & Self-Trail n. comb.
Braarudosphaera bigelowii (Gran & Braarud, 1935) Deflandre, 1947
Campylosphaera dela (Bramlette & Sullivan, 1961) Hay & Mohler, 1967
Cepkiella lumina (Sullivan, 1965) Bybell, 1975
Chiasmolithus bidens (Bramlette & Sullivan, 1961) Hay & Mohler, 1967
Chiasmolithus consuetus (Bramlette & Sullivan, 1961) Hay & Mohler, 1967
Chiasmolithus eograndis Perch-Nielsen, 1971
Coccolithus cribellum (Bramlette & Sullivan, 1961) Stradner, 1962
Coccolithus pelagicus (Wallich, 1877) Schiller, 1930
Cruciplacolithus tenuis (Stradner, 1961) Hay & Mohler in Hay et al., 1967
Cyclagelosphaera prima (Bukry, 1969) Bybell & Self-Trail, 1995
Discoaster anartios Bybell & Self-Trail, 1995
Discoaster araneus Bukry, 1971
Discoaster barbadiensis Tan Sin Hok, 1927
Discoaster binodosus Martini, 1958
Discoaster diastypus Bramlette & Sullivan, 1961
Discoaster falcatus Bramlette & Sullivan, 1961
Discoaster kuepperi Stradner, 1959
Discoaster lenticularis Bramlette & Sullivan, 1961
Discoaster limbatus Bramlette & Sullivan, 1961
Discoaster lodoensis Bramlette & Riedel, 1954
Discoaster mediosus Bramlette & Sullivan, 1961
Discoaster mohleri Bukry & Percival, 1971
Discoaster multiradiatus Bramlette & Riedel, 1954
Discoaster salisburgensis Stradner, 1961
Discoaster splendidus Martini, 1960
Ellipsolithus distichus (Bramlette & Sullivan, 1961) Sullivan, 1964
Ellipsolithus macellus (Bramlette & Sullivan, 1961) Sullivan, 1964
Ericsonia fenestrata (Deflandre & Fert, 1954) Stradner in Stradner and Edwards, 1968
Ericsonia subpertusa Hay & Mohler, 1967
Fasciculithus alanii Perch-Nielsen, 1971
Fasciculithus aubertae Haq & Aubry, 1981
Fasciculithus involutus Bramlette & Sullivan, 1961
Fasciculithus schaubii Hay & Mohler, 1967
Fasciculithus sidereus Bybell & Self-Trail, 1995
Fasciculithus thomasi Perch-Nielsen, 1971
Fasciculithus tympaniformis Hay & Mohler in Hay et al., 1967
Goniolithus fluckigeri Deflandre, 1957
Heliolithus riedelii Bramlette & Sullivan, 1961
Heliolithus universus Wind & Wise, 1976
Holodiscolithus macroporus (Deflandre in Deflandre and Fert, 1954) Roth, 1970
Holodiscolithus solidus (Deflandre in Deflandre and Fert, 1954) Roth, 1970
Hornibrookina arca Bybell & Self-Trail, 1995
Lophodolithus nascens Bramlette & Sullivan, 1961
Markalius apertus Perch-Nielsen, 1979
Markalius inversus Bramlette & Martini, 1964
Micrantholithus aequalis Sullivan, 1964
Micrantholithus inaequalis Martini, 1961
Micrantholithus pinguis Bramlette & Sullivan, 1961
Neochiastozygus concinnus (Martini, 1961) Perch-Nielsen, 1971
Neochiastozygus imbrii Haq & Lohmann, 1975
Neococcolithus dubius (Deflandre in Deflandre and Fert, 1954) Black, 1967
Neococcolithes protenus (Bramlette & Sullivan, 1961) Black, 1967
Placozygus sigmoides (Bramlette & Sullivan, 1961) Romein, 1979
Rhomboaster bramlettei (Brönnimann & Stradner, 1960) Bybell & Self-Trail, 1995
Rhomboaster contortus (Stradner, 1958) Bybell & Self-Trail, 1995
Rhomboaster digitalis (Aubry, 1996) Bybell & Self-Trail n. comb.
Rhomboaster orthostylus (Shamrai, 1963) Bybell & Self-Trail, 1995
Rhomboaster spineus (Shafik & Stradner, 1971) Perch-Nielsen, 1984
Rhomboaster weii Bybell & Self-Trail n. sp.
Scapholithus apertus Hay & Mohler, 1967
Scapholithus fossilis Deflandre in Deflandre and Fert, 1954
Sphenolithus anarrhopus Bukry & Bramlette, 1969
Sphenolithus conspicuus Martini, 1976
Sphenolithus editus Perch-Nielsen, 1978
Sphenolithus primus Perch-Nielsen, 1971
Sphenolithus radians Deflandre in Grasse, 1952
Toweius callosus Perch-Nielsen, 1971
Toweius eminens var. *eminens* (Bramlette & Sullivan, 1961) Gartner, 1971
Toweius eminens var. *tovae* Bybell & Self-Trail, 1995
Toweius occultatus (Locker, 1967) Perch-Nielsen, 1971
Toweius pertusus (Sullivan, 1965) Romein, 1979
Toweius serotinus Bybell & Self-Trail, 1995
Transversopontis pulcher (Deflandre in Deflandre and Fert, 1954) Perch-Nielsen, 1967
Transversopontis pulcheroides (Sullivan, 1964) Baldi-Beke, 1971
Zygodiscus herlyni Sullivan, 1964
Zygrhablithus bijugatus (Deflandre in Deflandre and Fert, 1954) Deflandre, 1959



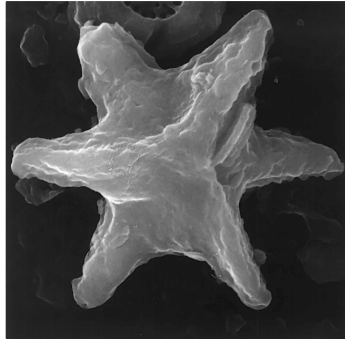
1



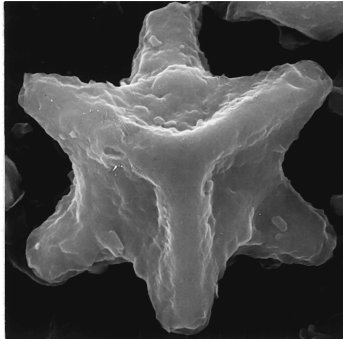
2



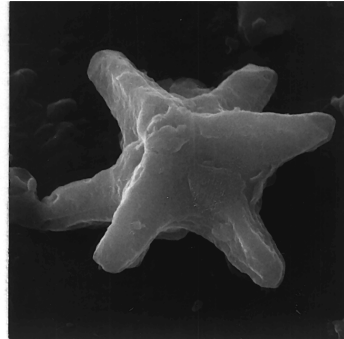
3a



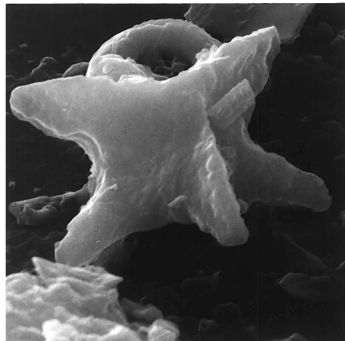
4a



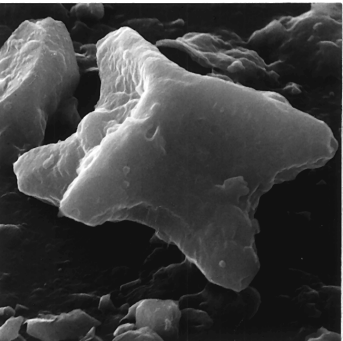
5a



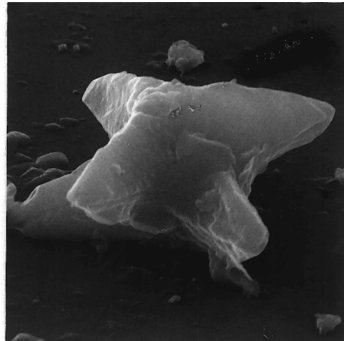
3b



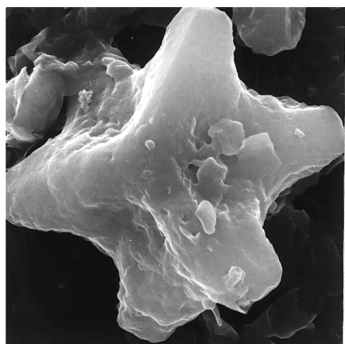
4b



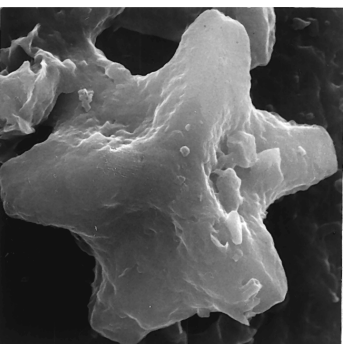
5b



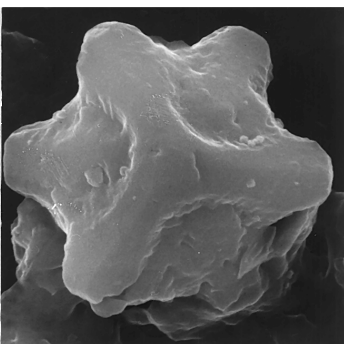
6



7a

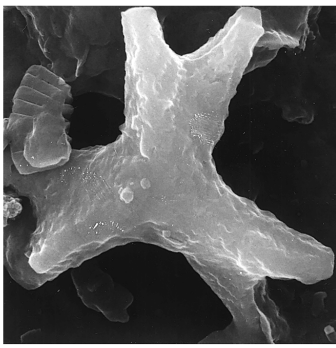


7b

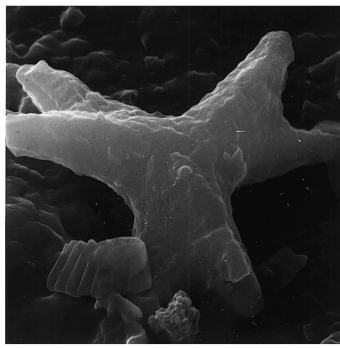


8

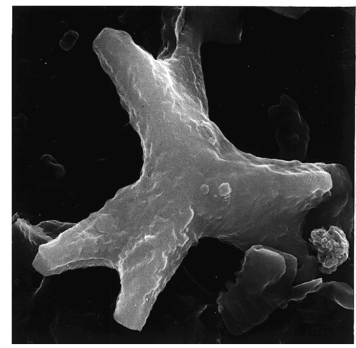
Plate 1. Island Beach Borehole 150X, New Jersey. All figures are SEM photomicrographs of *Rhomboaster bramlettei*. 1. 1066.9 ft, 4400X, Zone NP10. 2. 1066.9 ft, 4400X, Zone NP10. 3a. 1020.9 ft, 4400X, Zone NP10. 3b. Same specimen, tilted and rotated view. 4a. 1027.9 ft, 5400X, Zone NP10. 4b. Same specimen, tilted and rotated view. 5a. 1027.9 ft, 5400X, Zone NP10. 5b. Same specimen, tilted and rotated view. 6. 1020.9 ft, 4800X, Zone NP10. 7a. 1020.9 ft, 5200X, Zone NP10. 7b. Same specimen, tilted and rotated view. 8. 1020.9 ft, 6600X, Zone NP10.



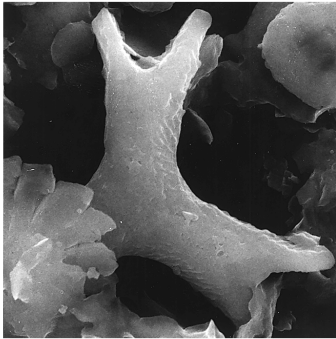
1a



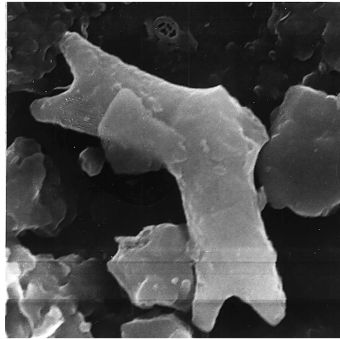
1b



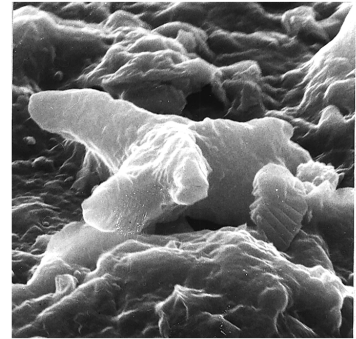
2a



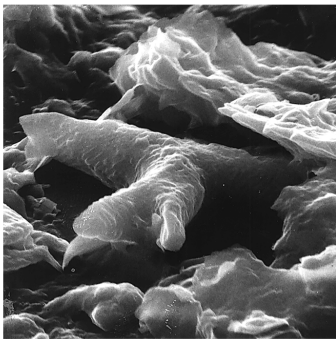
3a



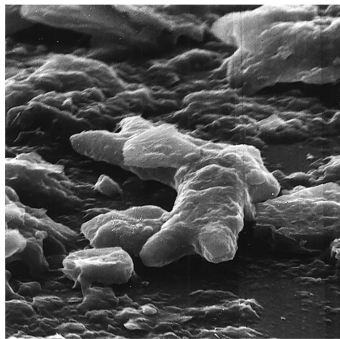
4a



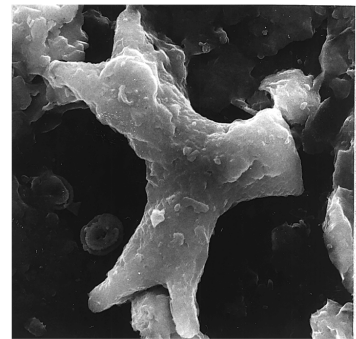
2b



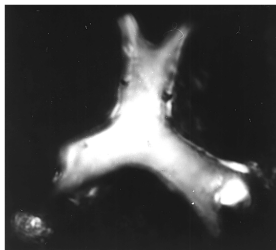
3b



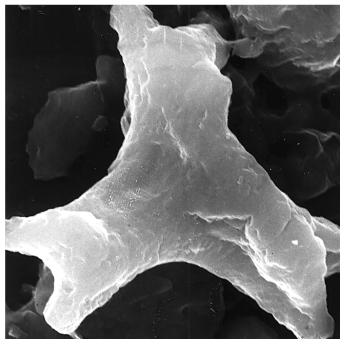
4b



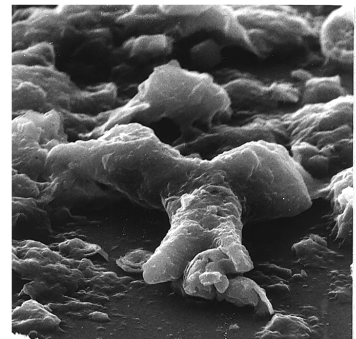
5a



6



7



5b

Plate 2. Island Beach Borehole 150X, New Jersey. All figures are SEM photomicrographs except Figure 6, which was photographed with cross-polarized light. Figures 1–2 are *Rhomboaster contortus*. **1a.** 1018.9 ft, 6000 \times , Zone NP10. **1b.** Same specimen, tilted view. **2a.** 1018.9 ft, 5400 \times , Zone NP10. **2b.** Same specimen, tilted view. Figures 3–7 are *Rhomboaster digitalis* n. comb. **3a.** 1073.9 ft, 4000 \times , Zone NP10. **3b.** Same specimen, tilted view. **4a.** 1059.9 ft, 3000 \times , Zone NP10. **4b.** Same specimen, tilted view. **5a.** 1073.9 ft, 2400 \times Zone NP10. **5b.** Same specimen, tilted view. **6.** 1075.2 ft, 2000 \times , Zone NP10. **7.** 1073.9 ft, 4400 \times , Zone NP10.

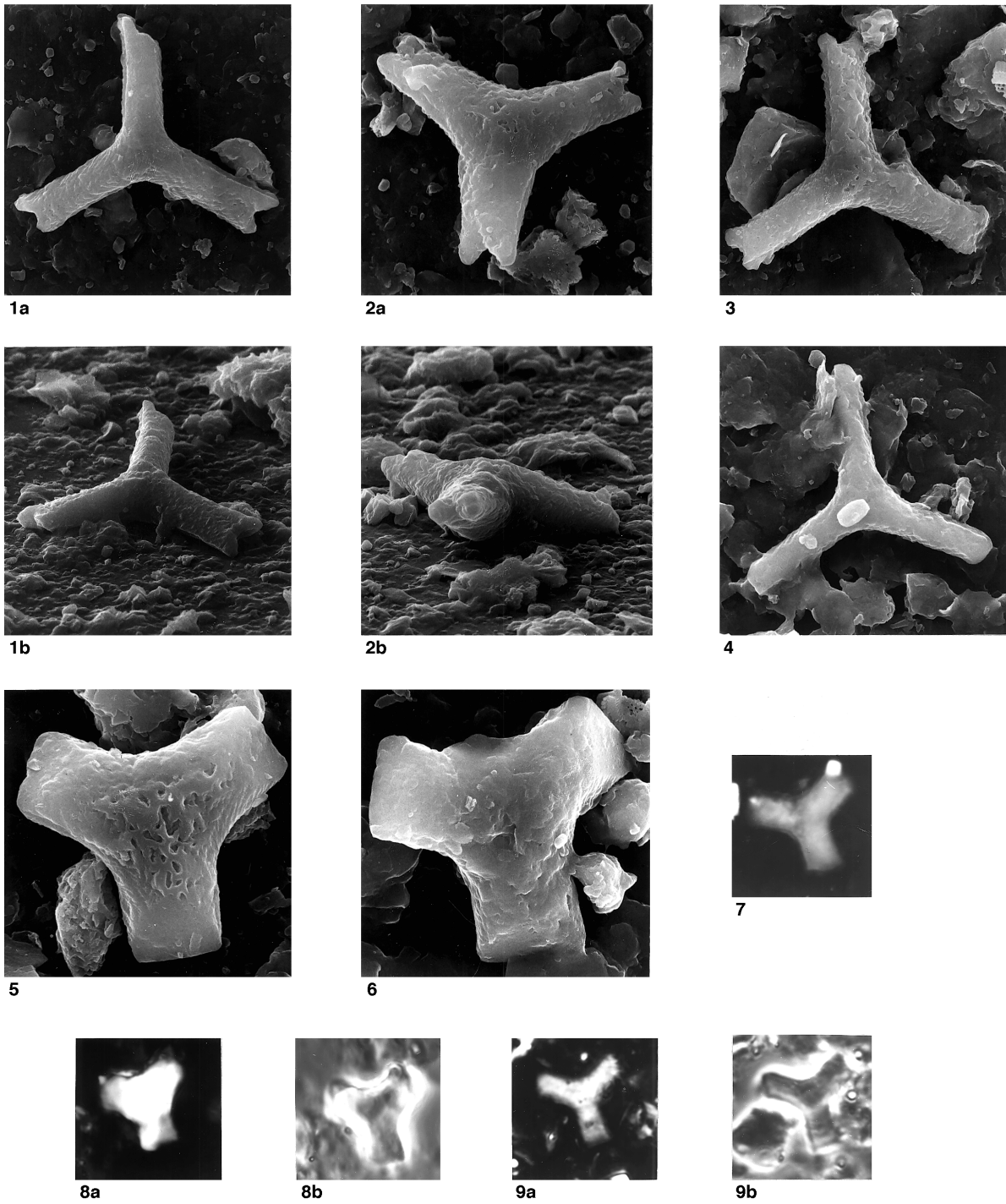


Plate 3. Island Beach Borehole 150X, New Jersey. Figures 1–6 are SEM photomicrographs. Figures 7, 8a, and 9a were photographed with cross-polarized light, and Figures 8b and 9b were photographed with phase-contrast light. Figures 1–4 are *Rhomboaster orthostylus*. **1a.** 1016.9 ft, 2600X, Zone NP11. **1b.** Same specimen, tilted view. **2a.** 1016.9 ft, 3200X, Zone NP11. **2b.** Same specimen, tilted view. **3.** 1016.9 ft, 2400X, Zone NP11. **4.** 1016.9 ft, 4000X, Zone NP11. Figures 5–9 are *Rhomboaster weii* n. sp. **5.** 1016.9 ft, 4400X, Zone NP11, holotype. **6.** 1073.9 ft, 4000X, Zone NP10, paratype. **7.** 1075.2 ft, 2000X, Zone NP10. **8a.** 1075.2 ft, 2000X, Zone NP10. **8b.** Same specimen, phase contrast. **9a.** 1075.2 ft, 2000X, Zone NP10. **9b.** Same specimen, phase contrast.

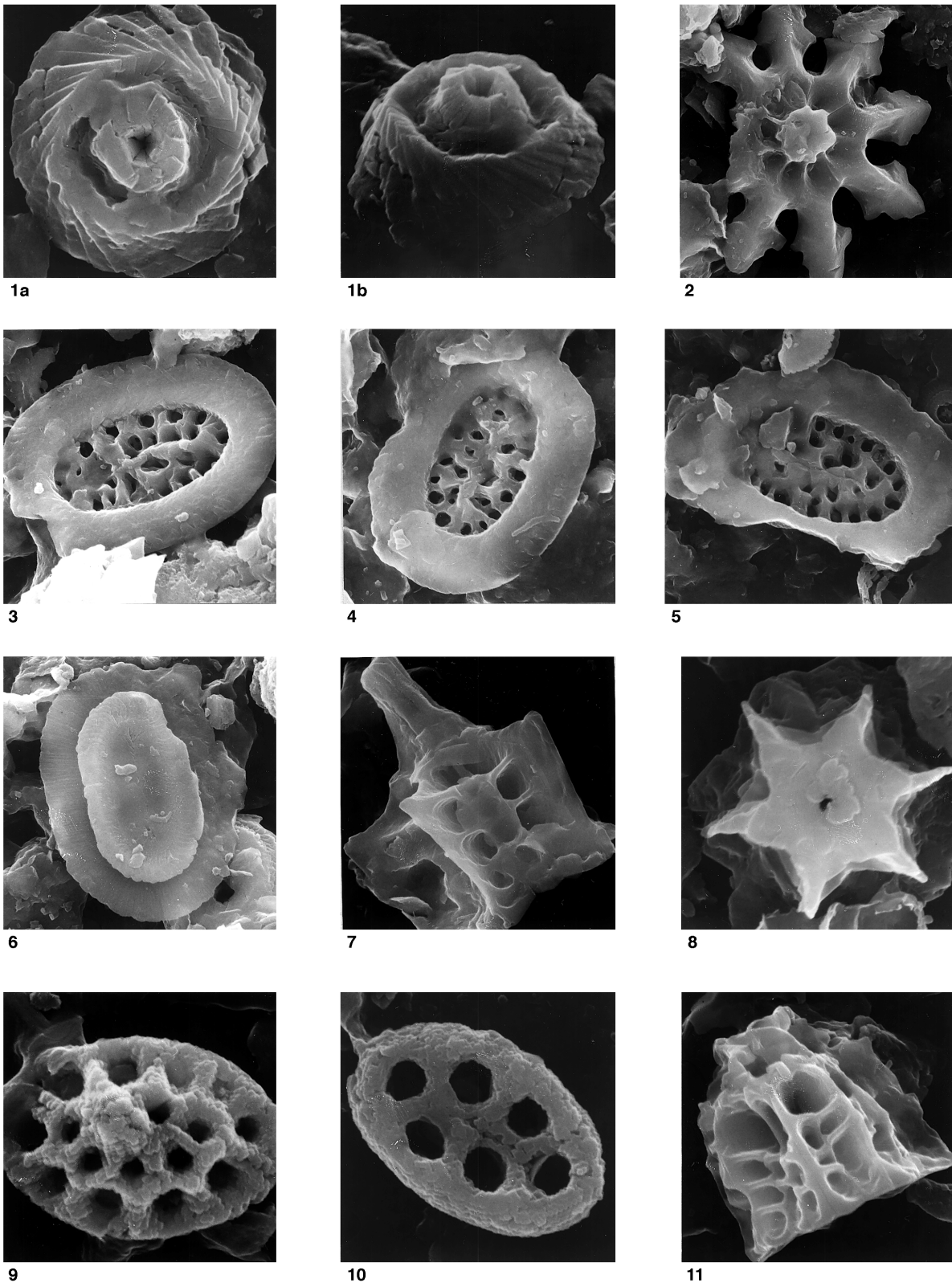
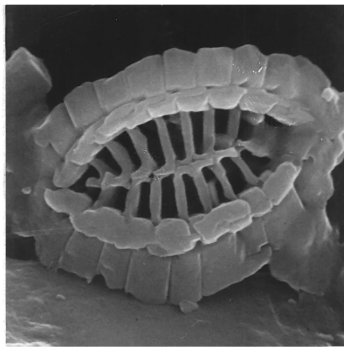
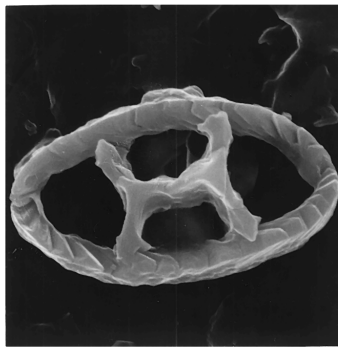


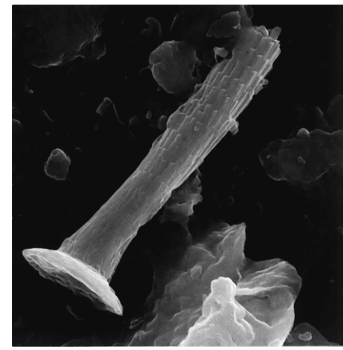
Plate 4. Island Beach Borehole 150X, New Jersey. All figures are SEM photomicrographs. **1a.** *Cyclagelosphaera prima*, 1073.9 ft, 10,000 \times , Zone NP10. **1b.** Same specimen, tilted view. **2.** *Discoaster limbatus*, 1023.8 ft, 4000 \times , Zone NP10. **3.** *Ellipsolithus* sp., 1018.9 ft, 4400 \times , Zone NP10. **4.** *Ellipsolithus* sp., 1018.9 ft, 4000 \times , Zone NP10. **5.** *Ellipsolithus* sp., 1018.9 ft, 4400 \times , Zone NP10. **6.** *Ellipsolithus macellus*, 1023.8 ft, 4800 \times , Zone NP10. **7.** *Fasciculithus schaubii*, 1059.9 ft, 6000 \times , Zone NP10. **8.** *Fasciculithus sidereus*, 1073.9 ft, 10,000 \times , Zone NP10. **9.** *Holodiscolithus macroporus*, 1018.9 ft, 12,000 \times , Zone NP10. **10.** *Holodiscolithus solidus*, 1020.9 ft, 10,000 \times , Zone NP10. **11.** *Fasciculithus thomasi*, 1023.8 ft, 8600 \times , Zone NP10.



1



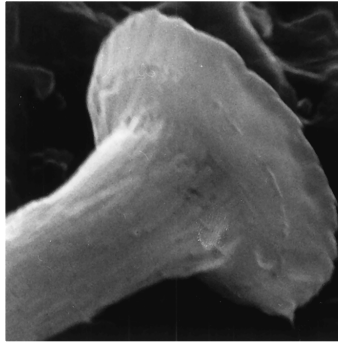
2



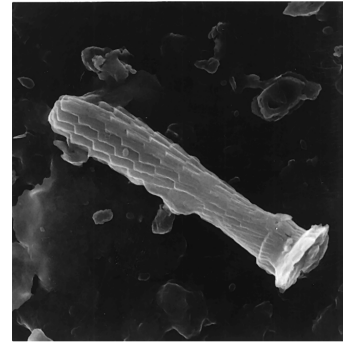
3



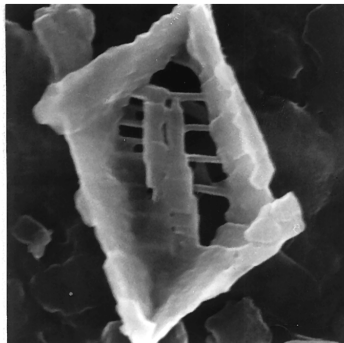
4



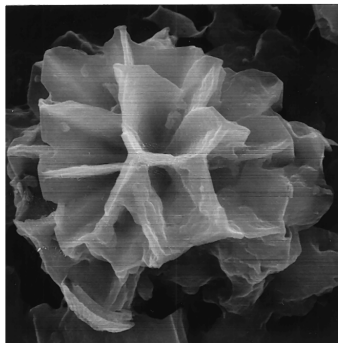
5



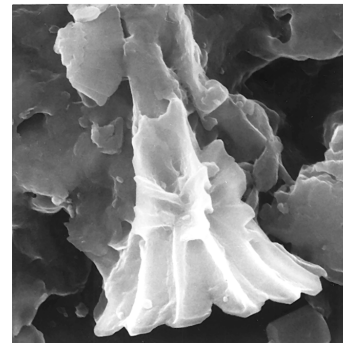
6



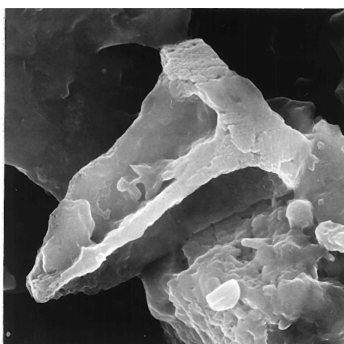
7



8



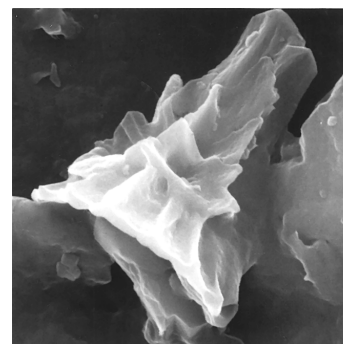
9



10



11



12

Plate 5. Island Beach Borehole 150X, New Jersey. All figures are SEM photomicrographs. 1. *Hornibrookina arca*, 1020.9 ft, 10,000X, Zone NP10. 2. *Neococolithes dubius*, 1018.9 ft, 7200X, Zone NP10. 3. *Blackites herculesii* n. comb., 1018.9 ft, 4000X, Zone NP10. 4. *Blackites herculesii* n. comb., 1018.9 ft, 10,000X, Zone NP10. 5. *Blackites herculesii* n. comb., 1018.9 ft, 12,000X, Zone NP10. 6. *Blackites herculesii* n. comb., 1059.9 ft, 4400X, Zone NP10. 7. *Scapholithus apertus*, 1023.8 ft, 12,000X, Zone NP10. 8. *Sphenolithus primus*, 1018.9 ft, 4800X, Zone NP10. 9. *Sphenolithus editus*, 1018.9 ft, 5400X, Zone NP10. 10. *Zygrhablithus bijugatus*, 1018.9 ft, 6000X, Zone NP10. 11. *Transversopontis pulcher*, 1018.9 ft, 7200X, Zone NP. 12. *Sphenolithus editus*, 1018.9 ft, 10,000X, Zone NP10.